SHELL-LATTICE CONSTRUCTION BASED ON REGULAR AND SEMI-REGULAR TILING VIA FUNCTIONAL COMPOSITION

Sumita Dahiya[1], Avi Shein[2] and Gershon Elber[3]

[1]Department of Computer Science, Technion, Israel; [1]sdahiya@campus.technion.ac.il,
[2] Tufts University
[3]Department of Computer Science, Technion, Israel

November 3, 2021

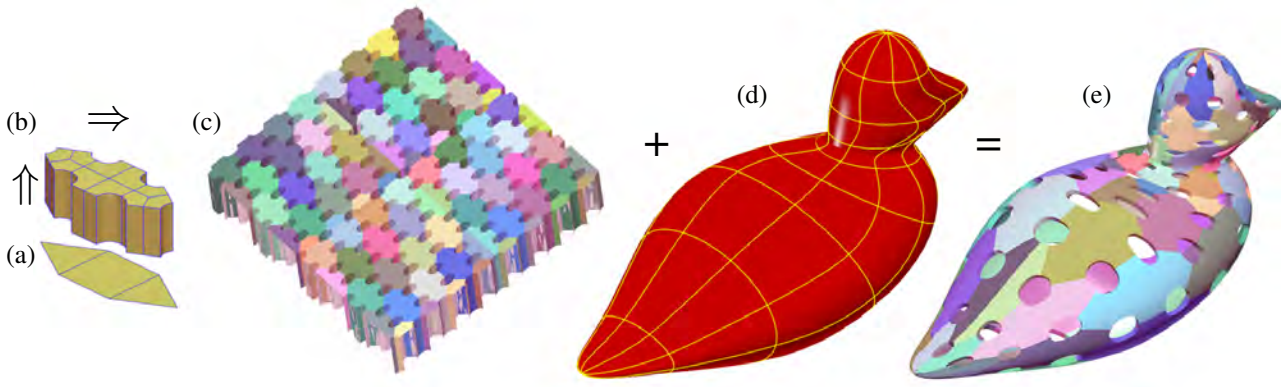

Figure 1: (a) Primal Semi-regular tile 43433. (b) Its dual tile 43433. (c) Periodically tessellated domain $[0, 1]^2$ using dual tile 43433, and randomly colored tiles. (d) Ruled shell volume between the duck surface and its offset. (e) Domain (c) is functionally composed into (d), yielding a shell-lattice structure.

ABSTRACT

This manuscript outlines a methodology and algorithm for the design of shell-lattice structures based on dual regular and semi-regular planar shapes. It introduces a 2-manifold, parametric freeform shell type of tiling to tessellate the domain of any given bivariate deformation map. The tessellated domain is functionally composed into the deformation map to obtain freeform shell-lattice structures in 3-space. Given any primal regular or semi-regular pattern, intrinsic controls over the thickened parameters of the dual graph are provided, results in a variety of tilings that differs in both physical properties and aesthetic appearance. Curve, surfaces, and trivariate tilings are offered, allowing analysis, optimization and fabrication of the shell-lattice results. This work concludes with several results from the implementation of the algorithms, including of 3D printed parts.

1 Introduction

1.1 Problem and Context

Regular prisms such as rectangular or cubical blocks are still the most used geometries to build up volume or shell structures, credit goes to their availability and ease of manufacturing. Architects and designers aim to obtain a prominent design space that consists of unconventional modular building blocks allowing variations in geometric, topological and

material properties. To achieve that, along with optimization of the geometry, topology and materials, a more systematic investigation is required in this direction.

For obtaining reliable and robust structures, there is a need for simple and formal approaches that provide intuitive designs and intrinsic control of a wide variety of modular building blocks. In this work, we introduce a dual version of semi-regular tiles which can be used to design and model intricate 2D lattice tiles. In the proposed approach, shell-lattice structures are obtained by functionally composing these dual (semi-) regular tiles and some deformation map. This dissociation between the micro and macro lattice structures provides the end users with a simplified and intuitive control over the design space and parameters. A simple yet flexible framework has been devised which can be effectively harnessed for modeling, designing, optimizing, and fabricating tile-able building blocks, in a variety of shell structures.

1.2 Inspiration and approach

Now a days, a wide variety of artifacts with intriguing and intricate properties can be fabricated with much ease, given the advancement achieved in additive manufacturing techniques. Use of heterogeneity and composites has expanded the manufacturing capabilities manifolds and opened up new frontiers to explore, for almost every industry. The approach proposed in this work leads to the construction of shell structures while optimizing the physical properties of the structures with respect to their geometry or their material, for example, striving for a high strength to weight ratio. Lattice structures are typically constructed using one or more unit cells that are periodic in nature and can be tessellated along any given axis [7]. Thin-shell or simply shell structures are lightweight constructions, made of typically shell (skin-like) elements, and are typically curved. These elements are then assembled to make large shell structures. The shell-lattice structures can widely be used in various industries, like automotive, aerospace and ship-building industries. These industries rely heavily on computer aided design to design structures and analyze their different physical behaviors, e.g. heat, fluid flow, or stress. Our goal is to construct these shell like structures and characterize their properties in a concise and intuitive way so as to allow for an informed exploration of the design space.

The foundation approach for the presented research work is the functional composition of the 2-manifold deformation map and the domain of the deformation map using copies of a dual (semi-) regular tile, i.e. functional composition [4, 10] of a given deformation map, $\tau : \mathbb{R}^2 \to \mathbb{R}^3$ and a tile, $T \in \mathbb{R}^2$, algebraically computing $\tau(T)$, i.e. image of T through τ.

1.3 Contributions

(i) A design space of 2D tilings based on dual regular and semi-regular tessellations of the plane, with results that are aesthetically pleasing.

(ii) Families of 2D tilings that can create shell-lattice structures of 3D geometries, while supporting analysis, optimization and fabrication of the same, with respect to the geometry, topology, and material/heterogeneity.

The rest of the paper is organized as follows. In Section 2, we survey related previous work. Then, Section 3 describes our entire algorithm to populate a general bivariate deformation map with tiles. Some examples and results are presented in Section 4, only to conclude in Section 5.

2 Related Work

Lattice-shell structures, widely exploited in civil, transportation and aerospace engineering, among others, are not always regular three dimensional structures nor planar. These thin wall structures like sandwich panels [17] and cylindrical shells with lattice cores [16] characterized by excellent mechanical and thermal properties, are used, for example, as draw tubes of space telescope, support structure of antenna in satellites and space platforms [22, 1]. Design and analysis of lattice-shells has gained a lot of attention in recent times. Wei et al. [18] worked on example based texture synthesis algorithms and Dumas et al. [3] extended this work to on-surface texture synthesizer that can work on voxel shell around the surface. Their algorithm can synthesize carved patterns along any given surface that can be fabricated over fused-filament printers. They have targeted surfaces in the form of a triangulated mesh, and the input is a colored image with binary pattern map to be synthesized along the surface. Although both the approaches results in structural patterns along surfaces, in the present study, our inputs are a B-spline bivariate surface and a dual (semi-) regular tile, which can be consisting of univariate curves, bivariate surfaces (possibly tessellated into a polygonal mesh), or trivariates.

Geometric regularities have always been intriguing for researchers working in the field of architecture and shape modeling. These aesthetically pleasing geometries, in the form of 3D tilings can show complex mechanical behavior, with different patterns characterizing different properties like anisotropy, variable stiffness and heat conductivity, etc.

Tessellations in the plane have been intensively studied and worked upon in mathematics [11] as well as in graphics [9]. Schumacher et al. [13] studied the mechanical properties of different polygonal tiling, by fixing the input base material and 3D printing different pattern prototypes. In their work, the sheet material is a thin extrusion of two-dimensional tilings. Minimal tileable units are identified and mapped to cylinders to study bending deformations corresponding to uniaxial curvature.

Trautz et al. [15] used regular, irregular and freeform geometries for the construction of shell and spatial structures based on the folded plate principle. They conclude that folding principle along with the freeform geometries can give rise to widely spanned light weight structures with high-strength. Weizmann et al. [19] experimentally studied the structural behavior of semi-regular and non regular topologically interlocking assemblies. They analyzed the structural performance based on the geometry and dimensions of topologically interlocking blocks. Given that each regular polygon is cyclic, Subramanian et al. [14] designed dual meshes relying on the cyclic properties of the regular and semi-regular tilings. A wide variety of artistic patterns of 2D tiling is shown by Kaplan [8], and Rao [12] has given an algorithm for construction of 2D pentagonal tiling.

Modeling constructor for micro-structures and porous geometries has been introduced by Elber [4] that can work for curve-trivariate, surface-trivariate and trivariate-trivariate function composition. By using 1-, 2- and 3-manifold based tiles and paving them multiple times inside the domain of a 3-manifold deforming trivariate function, smooth, precise and watertight, yet general, porous/micro-structure geometry might be constructed, via composition. Massarwi et al. [10] presented extensions to this micro-structure construction technique to construct fractal like heterogeneous, water-tight models with a high degree of precision.

Our presented work, in a sense, expands semi-regular planar tilings beyond tilings in 2D space to a rich design space of tilings in 3D space, while exploiting duality. Our goal is to construct shell-lattice structures, by utilizing the properties of semi-regular tilings, that can be studied and further utilized for, for instance, their mechanical and thermal characteristics. We aim to expand the design space that can be subjected to an informed exploration, and offer a continuum as families of such tilings, as univariate curves, bivariate surfaces, and trivariates shell elements, allowing for the design, analysis, optimization and fabrication of shell structures.

3 The algorithm

The space of regular and semi-regular tilings is partitioned into a set of distinct families, each of which admits certain tileability-preserving transformations on the shape of the tile. Parameterizing these shapes within a given family, can yield a continuous sub-space of patterns of the similar topology but potentially vastly different mechanical properties, for example solid-density[1], strength or heat conductivity.

This section is organized as follows: Section 3.1 presents the regular and semi-regular tiling topologies, and in Section 3.2, we discuss how the dual tile is constructed and controlled. In Section 3.2.1, we consider the tiling in the domain, tilings that are composed into the deformation function, as presented in Section 3.3.

3.1 Regular and semi-regular tilings

A tiling in the plane comprising of regular polygonal faces and isomorphic vertices, is commonly called as Euclidean regular tiling. Given that for a regular tiling (m, n), m is the number of sides in each face and n is the valence of vertices, there exists only three regular tilings characterized as $(3, 6)$, $(4, 4)$ and $(6, 3)$. In semi-regular tilings, more than one type of polygons exist, provided that the polygons are regular and all vertices have exactly the same structure of polygons around them. One naming convention of the different tilings stems from the types of polygons around each vertex where 3, 4, 6 denotes triangle, square and hexagon. For example, the semi regular tiling 44333 has two squares and three triangles around each vertex. There exists only eight semi-regular tilings summarized as $3636, 4346, 12312, 44333, 848, 43433, 1246$ and 333336, as shown in Figure 2.

3.2 Thickened dual semi-regular tilings

The notion of duality is one of the central concepts in geometry. It is generally defined in a very definite way using concrete structures. Duality is an existing property of geometric and algebraic structures which states that two concepts or operations can be used interchangeably, with both formulations holding the same results. The dual of a regular or a semi-regular tiling can be formed by considering center of each polygon as vertex and thereby joining the centers of adjacent polygons. The triangular and hexagonal tessellations are duals of each other, while the square tessellation is

[1] We define solid-density as the ratio of solid matter vs. air in the lattice, e.g. 100% is a full solid.

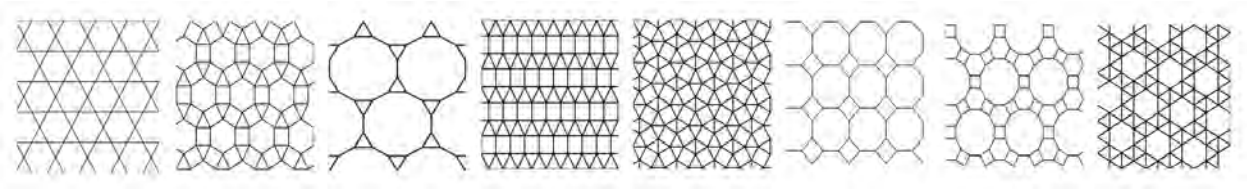

(6363) (4346) (12312) (44333) (43433) (848) (1246) (33336)

Figure 2: Semi-Regular tessellations.

its own dual. It is interesting to note that the dual of any given semi-regular tiling always consists of only one type of polygon and even that can be irregular. Duality allows the user to have a higher level of control over the shape pattern. And for some specific values of the control points the dual becomes the primal itself.

Our dual tiles of the semi-regular tiling are constructed by adding some thickness and curvature to the edges of the dual graph. This thickness is controlled by two additional parameters: a curvature sharpness (D_{curv}) of the thickened edges of the dual graph, and a fraction of the length of an edge in the primal tile (D_{frac}), where the thickened edge ends. Figure 3 shows a few examples, where we adjust D_{curv} and D_{frac}. One should note that if the value of D_{frac} = 0, D_{curv} holds no meaning. Also, if $D_{frac} = 1$ and D_{curv} = 1, the dual tile outlines the corresponding primal tile.

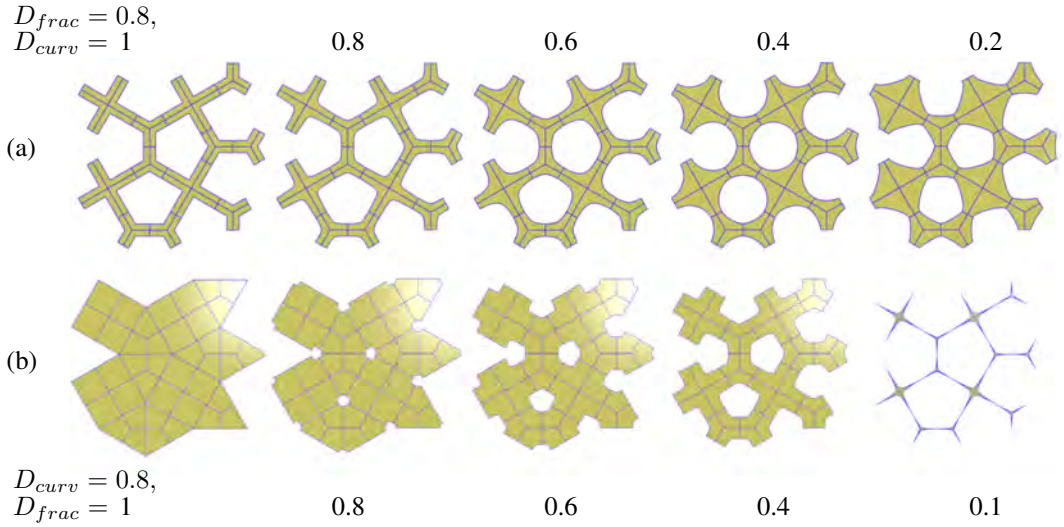

Figure 3: Visual variation in dual tile 43433 for (a) fixed value of D_{frac} and varying values of D_{curv} and (b) fixed value of D_{curv} and varying values of D_{frac}.

So far the tiles are merely univariate curves in the plane. However, we also allow surface and trivariate tiles. Surfaces are constructed by ruling opposite curves in the plane into planar surfaces, and trivariates are constructed by extruding the surfaces outside the plane to a desired elevation. See Figure 4.

3.2.1 Minimal tileable unit and lattice-tile

The minimal tileable units for planar tessellations, are the smallest translational units that can be paved across a 2D domain using translation operation only. See Figure 5, for minimal semi-regular tileable units, in black. The dual counterparts are shown in yellow color in Figure 5. Every tessellation shown in Figure 2 is built using one of these minimal tileable units or unit tiles. Each of these unit tiles create an infinite periodic tiling of the plane using translation only, emphasizing that (a regular or) a semi-regular tiling has translational periodicity.

3.3 Composing it all into a deformation map

Following [4], a tile is taken along with a deformation map. In this functional composition, we have used tiles that are either curves, or surfaces (possibly tessellated into a polygonal meshes), or trivariates, while the 2-manifold deforming function is a B-spline bi-variate surface. Clipping or bounding of the tiled domain is done by bringing both the tilings

(a)

(b)

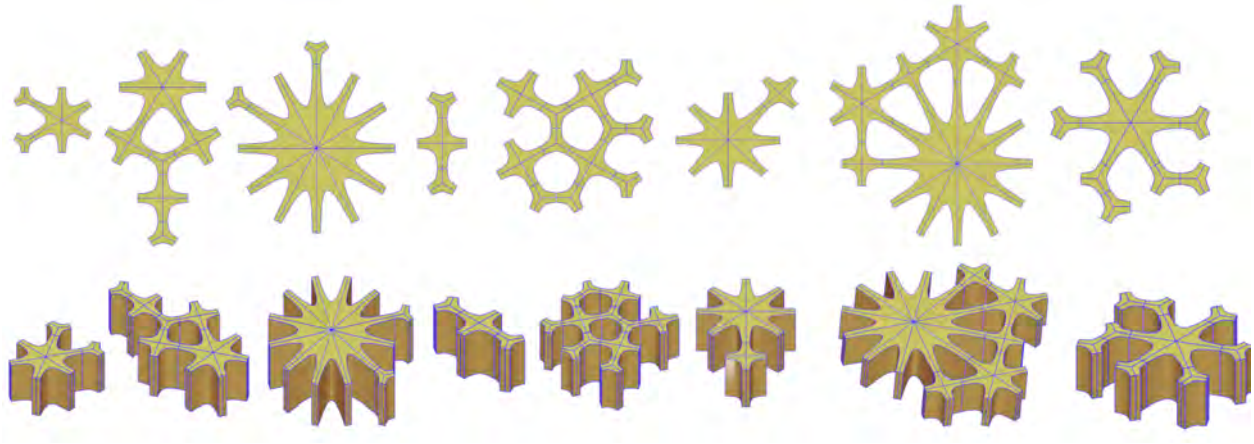

Figure 4: Given the univariate curves representing the dual tile, as in Figure 3, a planar surface representation for the tile is created by ruling opposite curves in the plane, as is seen in (a). By extruding the result of (a) outside the plane, trivariate tiles can be formed, as in (b). The order of the different tiles here is the same as in Figure 2, left to right.

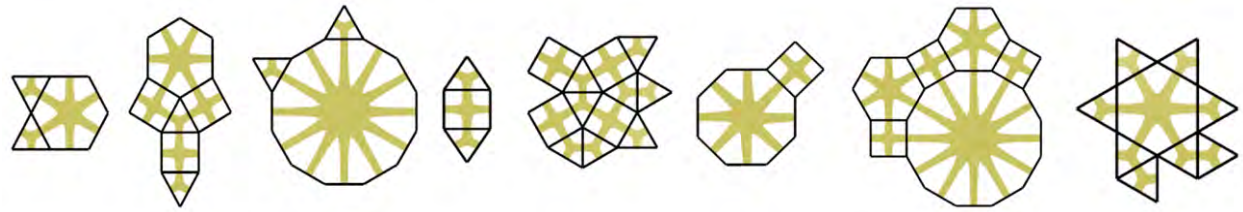

(6363) (4346) (12312) (44333) (43433) (848) (1246) (33336)

Figure 5: Minimal tileable units for Semi-regular tilings (in black) and the corresponding dual tiles (in yellow). The order of the different tiles here is the same as in Figures 2 and 4, left to right.

Algorithm 1 CreateDualTile - computes a dual tile of curves, given a primal tile.

Input:
T := a primal (semi-) regular tile, in R^2; ▷ Section 3.1
$TileSize$:= edge length of T;
D_{frac} := a fraction $\in [0, 1]$ of a primal edge;
D_{curv} := curvature sharpness of the thickened dual edges;
Output:
T_C := a (semi-) regular dual tile, of univariate curves, in R^2;
Algorithm:
1: $\mathcal{D}$:= the dual graph of T;
2: $T_C := \emptyset$
3: **for** every edge $E \in T$ **do**
4: $\{P_0, P_2\}$:= points on E with fraction $(D_{frac} : 1 - D_{frac})$ and $(1 - D_{frac} : D_{frac})$;
5: P_1 := point interior to T, between $\frac{P_0+P_2}{2}$ and closest location on $\mathcal{D}$, with ratio D_{curv};
6: C := A quadratic Bézier curve, using (P_0, P_1, P_2) as control points;
7: $T_C := T_C \cup \{C\}$;
8: **end for**
9: return T_C scaled to $TileSize$;

and the deforming function to domain $[0, 1]^2$. This clipping/bounding is done so to satisfy the condition that the tiled domain must be contained within the domain of the deformation map. Further, if the deformation function is closed or periodic, effort should be made to ensure the 2D tilings are also periodic along that edge. This entire process is summarized in Algorithm 1 and is depicted for a dual tile 44333 in Figure 1.

Algorithm 2 CreateShellLattice - computes a shell lattice, given a dual tile and the shell surface.

Input:
T_C := a (semi-) regular dual curve tile, in R^2; ▷ Algorithm 1
D := a bivariate deformation function, D: $R^2 \rightarrow R^3$;
$ShellThickness$:= offset amount to set the shell thickness;
Output:
$\mathcal{D}$:= A shell-lattice structure;
Algorithm:
1: $T_G := T_C$ either as curves, or elevated into surface- or trivariate-geometry; ▷ Section 3.2
2: $\mathcal{A}$:= arrangement of tile in $[0, 1]^2$, using T_G;
3: $\overline{D} := D$ Reparametrized to domain $[0, 1]^2$;
4: $\overline{D}_{ofst} := \overline{D}$ offset inside, by amount $ShellThickness$;
5: $\mathcal{D}_T$:= ruled trivariate between $\overline{D}$ and $\overline{D}_{ofst}$;
6: $\mathcal{D} := \mathcal{D}_T(\mathcal{A})$, the image of $\mathcal{A}$ through $\mathcal{D}_T$;
7: return $\mathcal{D}$;

4 Results

The definitions and algorithm described in the previous sections are implemented in the IRIT [5] solid modeling kernel. We hereby present some additional results from this implementation. All present results were created on an Intel Core i7-7700K 4.2 GHz PC with 32GB of main memory, and a single thread. Table 1 gives total time elapsed in the functional composition of the tiled domain for different 2-manifold deformation maps, constructed with different dual semi-regular tiles. A B-spline bivariate duck surface and the Utah teapot with four B-spline surfaces are considered.

Table 1: CPU time (in seconds) for the composition of different dual tiles with two deformation maps, a bivariate B-spline duck surface, an an Utah teapot with four B-spline surfaces.

Dual Tile	Duck, D_{frac} = 0.8, D_{curv} = 0.6	No. of Polygons composed in Duck	Teapot, D_{frac} = 0.8, D_{curv} = 0.6
44333	0.62, see Figure 6 (d)	349,088	3.31, see Figure 9 (d)
6363	1.20, see Figure 6 (a)	633,600	6.14, see Figure 9 (a)
33336	2.06, see Figure 6 (h)	1,030,080	10.15, see Figure 9 (b)
4346	2.28, see Figure 6 (b)	1,112,624	11.46, see Figure 9 (c)
43433	2.75, see Figure 6 (f)	1,339,968	13.51

Tiles comprising of curves, surfaces (possibly tessellated), or trivariates have been used, and randomly colored for clarity. The tiles shown in Figure 5 have been paved across the domain and then composed in the bivariate map 1 (d) to obtain the shell-lattice structures shown in Figure 6. Each tile in these shell-lattice structures is shown in different color, a practice that we exploit throughout. Figure 6 shows compositions for the different dual tiles. Each composition in Figure 6 varies in density depending lattice properties because of the varying density distribution of the different design patterns. The duck in Figure 6(c), constructed with tile 12312, shown in Figure 5, varies much in solid-density from the duck in Figure 6(d), constructed with tile 44333. Concurrent or local adjustment of the design patterns, material used and shell layer shapes or the deformation maps can be a deciding factor, for example, for the required mechanical or thermal characteristics of the final shell-lattice structures.

The algorithm results in shell-lattice structures that can have different solid-density. For a given deformation map, there are several ways to vary this solid-density: using a different topology, varying the D_{curv}, or varying D_{frac}. Figure 7 shows four different versions of the deformation map with dual tile 33336, for different values of D_{curv} and D_{frac}. Varying these parameters, results in shell-lattice structures that are significantly different from each other in appearance, solid-density and other physical properties, for example, strength, for the same topology. Similarly, in Figure 8, four shell-lattice structures are shown, made out from the dual tile 44333, by varying the values of the control parameters.

The algorithm is also verified on a different shell structure, comprising of a number of B-spline surfaces. Figure 9 shows four images of the Utah teapot constructed with four different dual tiles. Figure 10 shows two Utah teapots. For

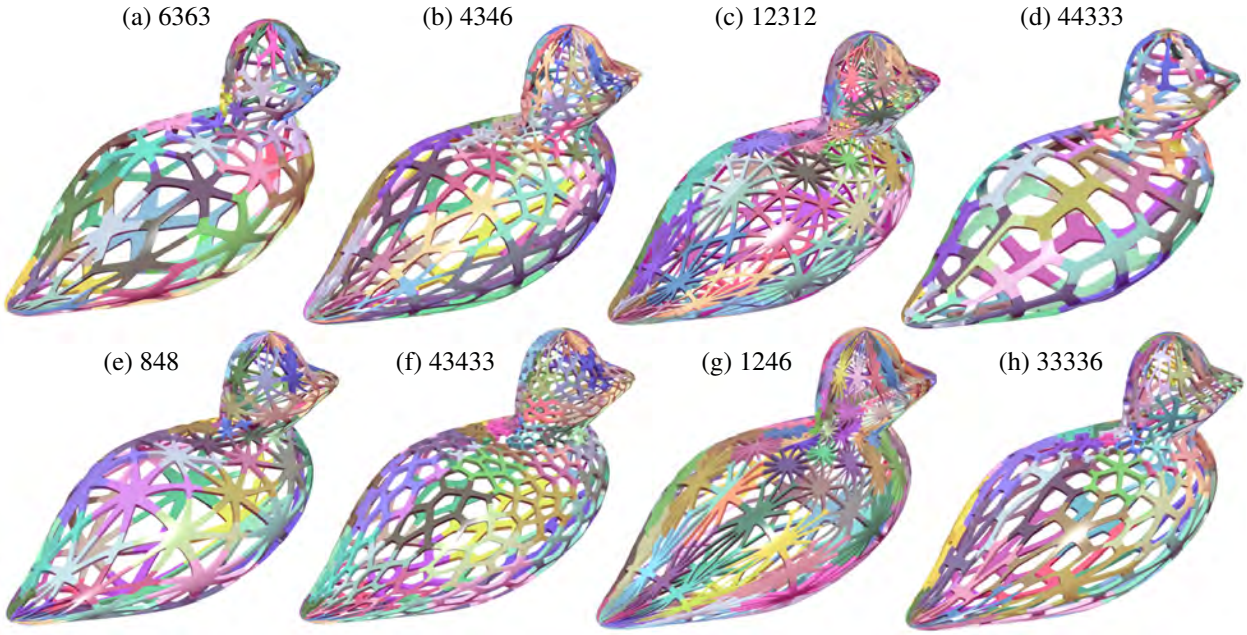

Figure 6: Different dual tiles composed into a duck surface.

each of the teapots, different parts of its body are composed with different dual tiles. In Figure 10 (a), the body of teapot is constructed using dual tile 44333, handle with dual tile 6363, spout with dual tile 43433 and lid with dual tile 33336. In 10 (b) dual tile 44333 used for body in 10 (a) is changed by the dual tile 4346. The proposed approach can be extended to shells with non-uniform thickness. Figure 11 demonstrates a tubular trivariate deformation map with a non-uniform thickness, shown in (a) and the composed non-uniform shell-lattice structure, composed with dual tiles 6363, shown in (b).

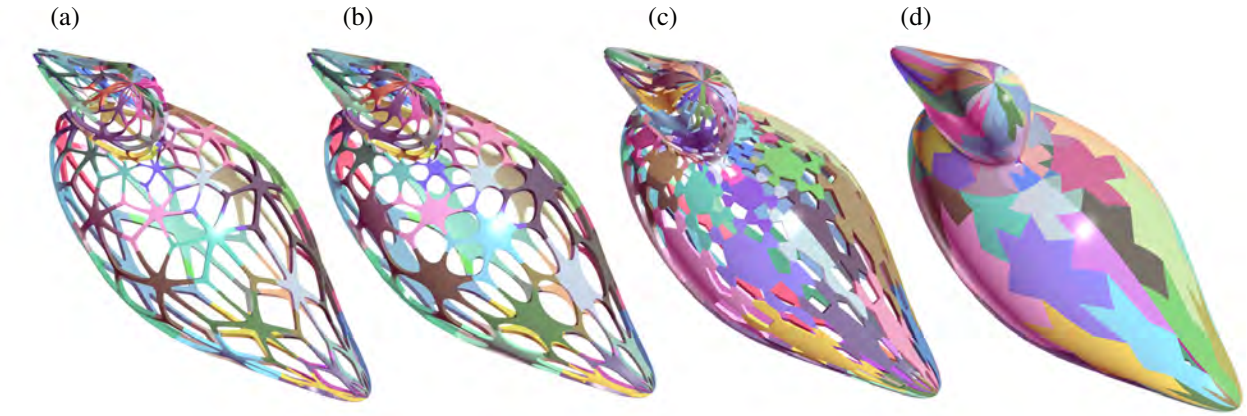

Figure 7: Tile 6363 (in (a) and (b)) and Tile 33336 (in (c) and (d)) composed into the duck surface for different values of D_{frac} and D_{curv}. (a) D_{frac} = 0.1 and D_{curv} = 0.9, (b) D_{frac} = 0.2 and D_{curv} = 0.5, (c) D_{frac} = 0.2 and D_{curv} = 0.1 and (d) D_{frac} = 1.0 and D_{curv} = 0.9

As stated in Section 3.2, we can construct trivariate dual tiles (recall Figure 4), and compose them into a trivariate deformation function to yield a trivariate volumetric representation of the shell structure. These trivariates can then be fed directly to analysis, using iso-geometric analysis [2]. Figure 12 shows one such example of a trivariate vase model composed with trivariate dual tilings based on 44333. Also shown in Figure 12 are hexa (cuboid) finite elements, that were sampled from these resulting trivariates, specifically in the Gmsh file format, and presented in the finite element software of Gmsh [6].

Finally, we present a pair of 3D printed model using geometry synthesized by the presented algorithms, in Figure 13. These models were tessellated into polygons and 3D printed on a J55 3D printer of Stratasys.

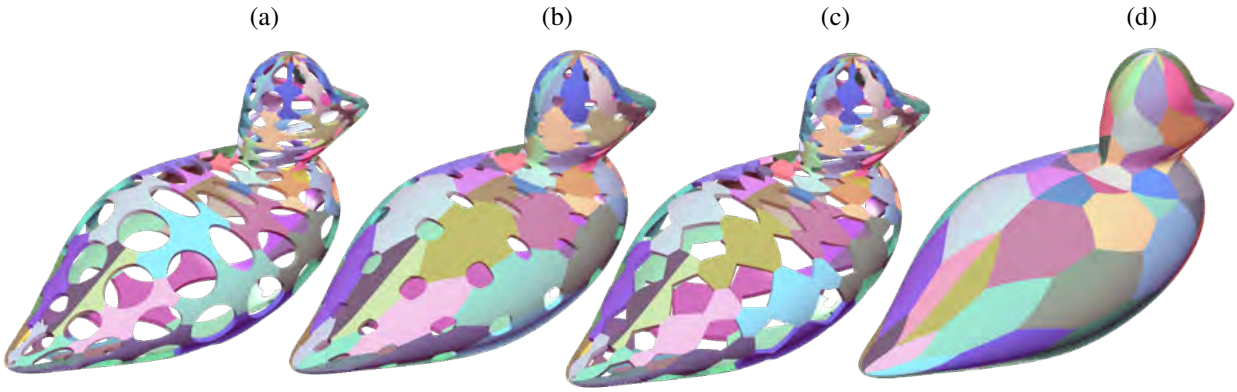

Figure 8: Tile 44333 shown in 5 (iv) composed into the duck surface for different values of D_{frac} and D_{curv}. (a) D_{frac} = 0.2 and D_{curv} = 0.4, (b) D_{frac} = 0.6 and D_{curv} = 0.6, (c) D_{frac} = 0.2 and D_{curv} = 0.0 and (d) D_{frac} = 1.0 and D_{curv} = 0.8

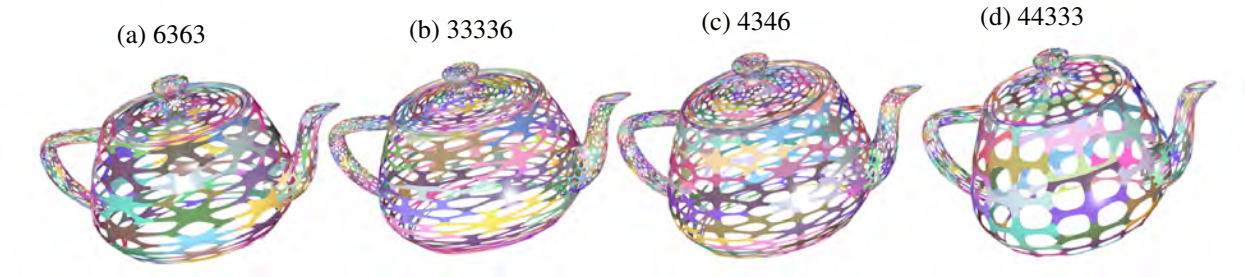

Figure 9: Different dual tiles composed into the Utah teapot surface. Dual tiles (a) 6363, (b) 33336, (c) 4346 (d) 44333 are used.

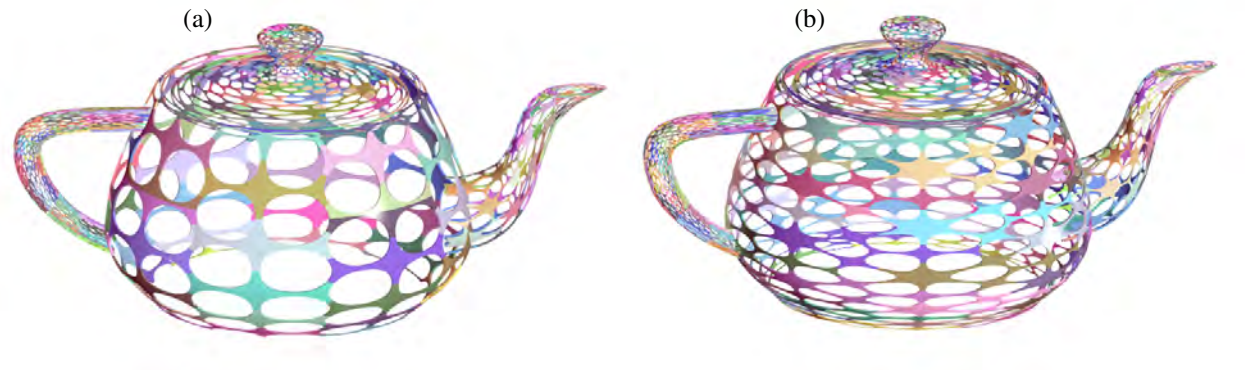

Figure 10: The different surfaces in the Utah teapot are composed with different tiles. In (a) body is made with dual tile 44333, handle with dual tile 6363, spout with dual tile 43433 and lid with dual tile 33336. In (b) body is changed to dual tile 4346.

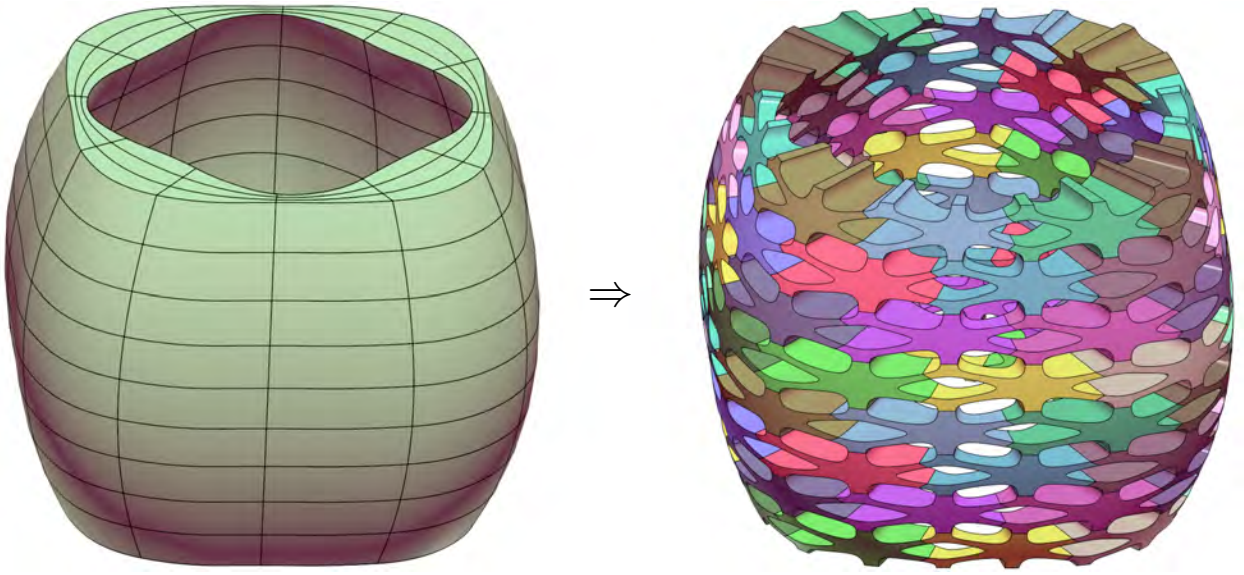

(a) (b)

Figure 11: (a) A tubular trivariate with non-uniform thickness and (b) shell-lattice structure of non-uniform thickness, composed with dual tile 6363, that result.

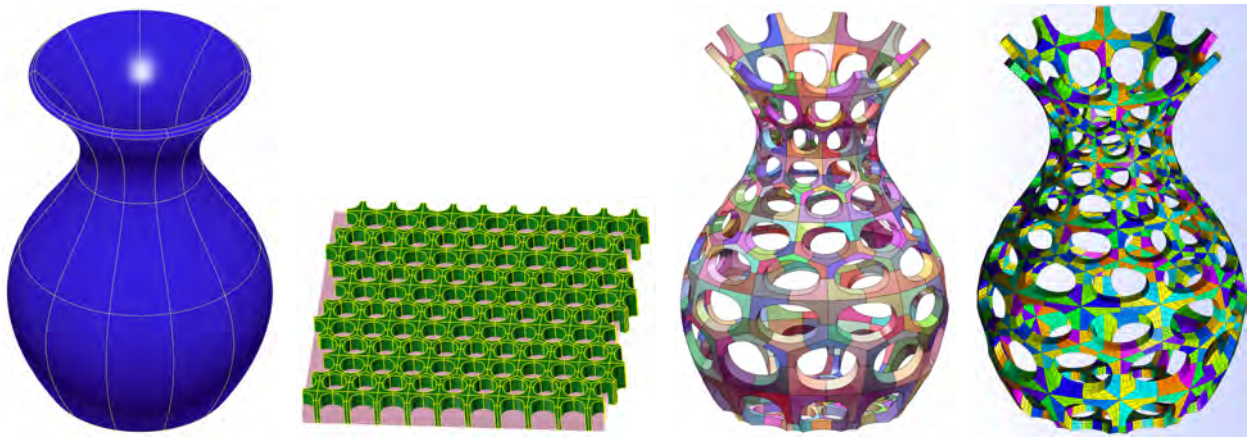

(a) (b) (c) (d)

Figure 12: A vase model in (a), is used to create a composition of tilings of a trivariate tile 44333 into it. (b) shows the $[0, 1]^2$ 2D tiling, extruded into trivariate tiles. In (c), the composed trivariates are shown in 3D. Finally, in (d), a finite element mesh, formed by a direct sampling of (c) into hexa (cuboid) finite elements is shown, via the Gmsh finite element software.

Figure 13: 3D printed samples. The duck is similar to the model in Figure 6 (a). The vase is the same geometry as in Figure 12. Printed on a J55 3D printer of Stratasys.

5 Conclusions and Future Work

While 2D tessellations and space filling shapes are relatively well-understood, problems related to 3D tessellations and space filling shapes are least exploited and potentially have applications in a wide range of areas including chemistry and biology to engineering and architecture. Possible future work includes:

1. Development of semi regular tessellations that are based on 3D space filling tilings and extend to micro-structure construction scheme with trivariate tiles, allowing the encoding of volumetric characteristics leading to heterogeneity.
2. Study and analysis of the physical behavior of the lattice structures built using various different patterns [20, 21].
3. Correlate between specific dual (semi-) regular lattices and desired physical properties while possibly fulfilling aesthetic criterion.
4. Support of trimmed surfaces. Here, the different dual tiles will be required to be clipped against the trimmed curves and stitched to neighboring tiles on the other adjacent surfaces, along these trimming curves.

6 Declaration of competing interest

The authors declare that they have no known competing financial interests or personal relationships that could have appeared to influence the work reported in this paper.

7 Acknowledgements

This research was supported in part by the ISRAEL SCIENCE FOUNDATION (grant No. 597/18) and in part with funding from the Defense Advanced Research Projects Agency (DARPA), under contract HR0011-17-2-0028. The views, opinions and/or findings expressed are those of the author and should not be interpreted as representing the official views or policies of the Department of Defense or the U.S. Government.

References

[1] CHEN, L., FAN, H., SUN, F., ZHAO, L., AND FANG, D. Improved manufacturing method and mechanical performances of carbon fiber reinforced lattice-core sandwich cylinder. *Thin-Walled Structures 68* (2013), 75–84.

[2] COTTRELL, J. A., HUGHES, T. J., AND BAZILEVS, Y. *Isogeometric analysis: toward integration of CAD and FEA*. John Wiley & Sons, 2009.

[3] DUMAS, J., LU, A., LEFEBVRE, S., WU, J., AND DICK, C. By-example synthesis of structurally sound patterns. *ACM Transactions on Graphics (TOG) 34*, 4 (2015), 1–12.

[4] ELBER, G. Precise construction of micro-structures and porous geometry via functional composition. In *International conference on mathematical methods for curves and surfaces* (2016), Springer, pp. 108–125.

[5] ELBER, G. The irit modeling environment, version 12. http://www.cs.technion.ac.il/~irit, 2021.

[6] GMSH. The gmsh finite element software. https://gmsh.info, 2021.

[7] HELOU, M., AND KARA, S. Design, analysis and manufacturing of lattice structures: an overview. *International Journal of Computer Integrated Manufacturing 31*, 3 (2018), 243–261.

[8] KAPLAN, C. S. Voronoi diagrams and ornamental design. In *Proceedings of the First Annual Symposium of the International Society for the Arts, Mathematics, and Architecture (ISAMA'99)* (1999), pp. 277–283.

[9] KAPLAN, C. S. Introductory tiling theory for computer graphics. *Synthesis Lectures on Computer Graphics and Animation 4*, 1 (2009), 1–113.

[10] MASSARWI, F., MACHCHHAR, J., ANTOLIN, P., AND ELBER, G. Hierarchical, random and bifurcation tiling with heterogeneity in micro-structures construction via functional composition. *Computer-Aided Design 102* (2018), 148–159.

[11] PAUFLER, P., GRÜNBAUM, B., AND SHEPHARD, G. Tilings and patterns. wh freeman and co. ltd., oxford 1987.

[12] RAO, M. Exhaustive search of convex pentagons which tile the plane,(2017), 2017.

[13] SCHUMACHER, C., MARSCHNER, S., GROSS, M., AND THOMASZEWSKI, B. Mechanical characterization of structured sheet materials. *ACM Transactions on Graphics (TOG) 37*, 4 (2018), 1–15.

[14] SUBRAMANIAN, S. G., ENG, M., KRISHNAMURTHY, V. R., AND AKLEMAN, E. Delaunay lofts: A biologically inspired approach for modeling space filling modular structures. *Computers & Graphics 82* (2019), 73–83.

[15] TRAUTZ, M., AND HERKRATH, R. The application of folded plate principles on spatial structures with regular, irregular and free-form geometries. In *Symposium of the International Association for Shell and Spatial Structures (50th. 2009. Valencia). Evolution and Trends in Design, Analysis and Construction of Shell and Spatial Structures: Proceedings* (2009), Editorial Universitat Politècnica de València.

[16] WANG, Z.-W., HAN, Q.-F., NASH, D. H., AND LIU, P.-Q. Investigation on inconsistency of theoretical solution of thermal buckling critical temperature rise for cylindrical shell. *Thin-Walled Structures 119* (2017), 438–446.

[17] WEI, K., HE, R., CHENG, X., ZHANG, R., PEI, Y., AND FANG, D. Fabrication and mechanical properties of lightweight zro2 ceramic corrugated core sandwich panels. *Materials & Design 64* (2014), 91–95.

[18] WEI, L.-Y., LEFEBVRE, S., KWATRA, V., AND TURK, G. State of the art in example-based texture synthesis. In *Eurographics 2009, State of the Art Report, EG-STAR* (2009), Eurographics Association, pp. 93–117.

[19] WEIZMANN, M., AMIR, O., AND GROBMAN, Y. J. Structural performance of semi-regular topological interlocking assemblies. In *Proceedings of the Symposium on Simulation for Architecture and Urban Design* (2019), pp. 1–7.

[20] ZHANG, X., FANG, G., DAI, C., VERLINDEN, J., WU, J., WHITING, E., AND WANG, C. C. Thermal-comfort design of personalized casts. In *Proceedings of the 30th Annual ACM Symposium on User Interface Software and Technology* (2017), pp. 243–254.

[21] ZHANG, X., LE, X., WU, Z., WHITING, E., AND WANG, C. C. Data-driven bending elasticity design by shell thickness. In *Computer Graphics Forum* (2016), vol. 35, Wiley Online Library, pp. 157–166.

[22] ZHAO, Y., CHEN, M., YANG, F., ZHANG, L., AND FANG, D. Optimal design of hierarchical grid-stiffened cylindrical shell structures based on linear buckling and nonlinear collapse analyses. *Thin-Walled Structures 119* (2017), 315–323.